

Magnetic phase diagram of the dimerized spin $S = \frac{1}{2}$ ladder

G.I. Japaridze¹ and S. Mahdavifar²

¹ Institut für Theoretische Physik, Universität zu Köln, Zùlpicher Str. 77, D-50937 Köln, Germany
and Andronikashvili Institute of Physics, Tamarashvili 6, 0177, Tbilisi, Georgia

² Department of Physics, University of Guilan, 41335-1914, Rasht, Iran

Received: March 6, 2022

Abstract. The ground-state magnetic phase diagram of a spin $S = 1/2$ two-leg ladder with alternating rung exchange $J_{\perp}(n) = J_{\perp}[1 + (-1)^n \delta]$ is studied using the analytical and numerical approaches. In the limit where the rung exchange is dominant, we have mapped the model onto the effective quantum sine-Gordon model with topological term and identified two quantum phase transitions at magnetization equal to the half of saturation value from a gapped to the gapless regime. These quantum transitions belong to the universality class of the commensurate-incommensurate phase transition. We have also shown that the magnetization curve of the system exhibits a plateau at magnetization equal to the half of the saturation value. We also present a detailed numerical analysis of the low energy excitation spectrum and the ground state magnetic phase diagram of the ladder with rung-exchange alternation using Lanczos method of numerical diagonalizations for ladders with number of sites up to $N = 28$. We have calculated numerically the magnetic field dependence of the low-energy excitation spectrum, magnetization and the on-rung spin-spin correlation function. We have also calculated the width of the magnetization plateau and show that it scales as δ^{ν} , where critical exponent varies from $\nu = 0.87 \pm 0.01$ in the case of a ladder with isotropic antiferromagnetic legs to $\nu = 1.82 \pm 0.01$ in the case of ladder with ferromagnetic legs. Obtained numerical results are in a complete agreement with estimations made within the continuum-limit approach.

PACS. 75.10.Jm Quantized spin models; 75.10.Pq Spin chain models

1 Introduction

Low-dimensional quantum magnetism has been the subject of intense research activity since the pioneering paper by Bethe [1]. Perpetual during the decades interest in study of these systems is determined by their remarkably rich and unconventional low-energy properties (see for review Ref. 2). An increased current activity in this field is connected with the large number of qualitatively new and dominated by the quantum effects phenomena discovered in these systems [3,4] as well as with the opened wide perspectives for use low-dimensional magnetic materials in modern nanoscale technologies.

The spin $S = 1/2$ two-leg ladders represent one, particular subclass of low-dimensional quantum magnets which also has attracted a lot of interest for a number of reasons. On the one hand, there was remarkable progress in recent years in the fabrication of such ladder compounds [5]. On the other hand, spin-ladder models pose interesting theoretical problems since antiferromagnetic two-leg ladder systems with spin $S = 1/2$ have a gap in the excitation spectrum [6,7,8] they reveal an extremely rich behavior, dominated by quantum effects in the presence of a magnetic field. These quantum phase transitions were

intensively investigated both theoretically [9-24] and experimentally [25-30].

Usually, these most exciting properties of low dimensional quantum spin systems exhibit strongly correlated effects driving them toward regimes with no classical analog. Properties of the systems in these regimes or "quantum phases" depend in turn on the properties of their ground state and low-lying energy excitations. Therefore search for the gapped phases emerging from different sources and study of ordered phases and quantum phase transitions associated with the dynamical generation of new gaps is an important direction in theoretical studies of quantum spin systems.

A particular realization of such scenario appears in the case where the spin-exchange coupling constants are spatially modulated. The spin-Peierls effect in spin chains represent prototype example of such behavior [31]. In the recent paper of one of the authors the new type of effective spin-Peierls phenomenon in ladder systems, connected with spontaneous dimerization of the system during the magnetization process via alternation of rung exchange has been discussed [32]. The Hamiltonian of the model is

$$\mathcal{H} = J_{\parallel} \sum_{n,\alpha} \mathbf{S}_{n,\alpha} \cdot \mathbf{S}_{n+1,\alpha} - H \sum_{n,\alpha} S_{n,\alpha}^z$$

$$+ J_{\perp} \sum_n [1 + (-1)^n \delta] \mathbf{S}_{n,1} \cdot \mathbf{S}_{n,2}, \quad (1)$$

where $\mathbf{S}_{n,\alpha}$ is the spin $S = 1/2$ operator of rung n ($n=1, \dots, L$) and leg α ($\alpha = 1, 2$). The interleg coupling is antiferromagnetic, $J_{\perp}^{\pm} = J_{\perp}(1 \pm \delta) > 0$.

In Ref. 32 the model was studied analytically in the limit of strong rung exchange and magnetic field $J_{\perp}^{\pm} \simeq H \gg |J_{\parallel}|, \delta J_{\perp}$. In this limit the ladder Hamiltonian is mapped onto the spin-1/2 XXZ Heisenberg chain in the presence of both longitudinal uniform and staggered magnetic fields, with the amplitude of the staggered component of the magnetic field proportional to $\sim \delta J_{\perp}^0$. The continuum-limit bosonization analysis of the effective spin-chain Hamiltonian show, that the alternation of the rung-exchange leads to the dynamical generation of a new energy scale in the system and to the appearance of two additional quantum phase transitions in the magnetic ground state phase diagram. These transitions manifest themselves most clearly in the presence of a new magnetization plateau at magnetization equal to one half of its saturation value. It was shown that the new commensurability gap (correspondingly the width of magnetization plateau) scales as δ^{ν} , where $\nu = 4/5$ in the case of a ladder with isotropic antiferromagnetic legs and $\nu = 2$ in the case of a ladder with isotropic ferromagnetic legs. Although up to now no materials are available which realize this models, theoretical studies of this type of Peierls distortion is extremely interesting, since such an instability could in principle develop during the magnetization process of an antiferromagnetic ladder, in particular with high probability in the case of applied uniaxial along legs pressure.

In this paper we continue our studies of an isotropic spin $S = 1/2$ two-leg ladder with alternating rung exchange in a uniform magnetic field using the numerical analysis. In particular we apply the Lanczos method to diagonalize numerically finite ladder systems with lengths $L = 6, 8, 10, 12, 14$. Using the exact diagonalization results, we calculate the spin gap, magnetization and the intra-rung spin correlations as a function of applied magnetic field. We have also calculated the spin-density distribution in the ground state at magnetization plateau. Based on the exact diagonalization results we obtain the ground-state magnetic phase diagram of the model showing four quantum phase transitions, in agreement with the predictions made in Ref. 32. We also numerically computed the width of the plateau and show it scales as δ^{ν} , where $\nu = 0.87 \pm 0.01$ in the case of a ladder with isotropic antiferromagnetic legs and $\nu = 1.82 \pm 0.02$ in the case of a ladder with isotropic ferromagnetic legs.

The paper is organized as follows. In the forthcoming section we briefly summarize results of the analytical studies. In section III, we present numerical results of our exact diagonalization studies of the system. Finally, we conclude and summarize our results in section IV.

2 Effective Hamiltonian

In this section we briefly summarize the results obtained within the analytical studies. To obtain the effective spin-

chain we follow the route already used to studies of the standard two-leg ladder models in the same limit of strong rung exchange [12,13]. We start from the case $J_{\parallel} = 0$, where the system decouples into a set of noninteracting rungs with couplings $J_{\perp}(n) = J_{\perp}[1 \pm (-1)^n \delta]$ and an eigenstate of the Hamiltonian is written as a product of rung states. At each rung, two spins form either a singlet state $|s\rangle$ with energy $E_s(n) = -0.75J_{\perp}(n)$ or in one of the triplet states $|t^+\rangle, |t^0\rangle$ and $|t^-\rangle$ with energies $E_{t^+}(n) = 0.25J_{\perp}(n) - H$, $E_{t^0}(n) = 0.25J_{\perp}(n)$ and $E_{t^-}(n) = 0.25J_{\perp}(n) + H$, respectively. When H is small, the ground state consists of a product of rung singlets. As the field H increases, the energy of the triplet state $|t^+\rangle$ decreases and at $H \simeq J_{\perp}(n)$ forms, together with the singlet state, a doublet of almost degenerate low energy state, split from the remaining high energy two triplet states. This allows to introduce the effective spin operator τ which act on these states as [12]

$$\begin{aligned} \tau_n^z |s_0\rangle_n &= -\frac{1}{2} |s_0\rangle_n, & \tau_n^z |t^+\rangle_n &= \frac{1}{2} |t^+\rangle_n, \\ \tau_n^+ |s_0\rangle_n &= |t^+\rangle_n, & \tau_n^+ |t^+\rangle_n &= 0, \\ \tau_n^- |s_0\rangle_n &= 0, & \tau_n^- |t^+\rangle_n &= |s_0\rangle_n. \end{aligned} \quad (2)$$

The relation between the real spin operator \mathbf{S}_n and the pseudo-spin operator $\boldsymbol{\tau}_n$ in this restricted subspace can be easily derived by inspection,

$$S_{n,\alpha}^{\pm} = (-1)^{\alpha} \frac{1}{\sqrt{2}} \tau_n^{\pm}, \quad S_{n,\alpha}^z = \frac{1}{2} \left(\frac{1}{2} + \tau_n^z \right). \quad (3)$$

Using (3), to the first order and up to a constant, we easily obtain the effective Hamiltonian

$$\begin{aligned} H_{eff} &= \sum_n \left\{ \frac{1}{2} J_{xy} (\tau_n^+ \tau_{n+1}^- + h.c.) + J_z \tau_n^z \tau_{n+1}^z \right\} \\ &\quad - h_{eff}^0 \sum_n \tau_n^z - h_{eff}^1 \sum_n (-1)^n \tau_n^z, \end{aligned} \quad (4)$$

where $J_{xy} = 2J_z = J_{\parallel}$ and

$$h_{eff}^0 = H - J_{\perp} - J_{\parallel}/2, \quad h_{eff}^1 = \delta J_{\perp}. \quad (5)$$

Thus the effective Hamiltonian is nothing but the XXZ Heisenberg chain, with anisotropy $J_z/J_{xy} \equiv \Delta = 1/2$ in a uniform and staggered longitudinal magnetic fields. It is worth to notice that a similar problem has been studied intensively in recent years [33,34,35,36,37].

2.1 The first critical field H_{c_1} and the saturation field H_{c_2}

The performed mapping allows to determine critical fields H_{c_1} corresponding to the onset of magnetization in the system and the saturation field H_{c_2} [12]. The easiest way to express H_{c_1} and H_{c_2} in terms of ladder parameters is to perform the Jordan-Wigner transformation which maps

the problem onto a system of interacting spinless fermions [38]:

$$H_{sf} = t \sum_n (a_n^+ a_{n+1} + h.c.) + V \sum_n \rho_n \rho_{n+1} - \sum_n [\mu_0 + (-1)^n \mu_1] \rho_n, \quad (6)$$

where $t = V = J_{\parallel}/2$, $\mu_0 = h_{eff}^0 + J_{\parallel}/2$ and $\mu_1 = h_{eff}^1$. The lowest critical field H_{c1} corresponds to that value of the chemical potential μ_{0c} for which the band of spinless fermions starts to fill up. In this limit we can neglect the interaction term in Eq. (6) and obtain the model of free massive particles with spectrum $E^{\pm}(k) = -\mu_0 \pm (J_{\parallel}^2 \cos^2(k) + \mu_1^2)^{1/2}$. This gives $H_{c1} = J_{\perp} - (J_{\parallel}^2 + \delta^2 J_{\perp}^2)^{1/2}$. A similar argument can be used to determine H_{c2} . In the limit of almost saturated magnetization, it is useful to make a particle-hole transformation and estimate H_{c2} from the condition where the transformed hole band starts to fill, what gives $H_{c2} = J_{\perp} + (J_{\parallel}^2 + \delta^2 J_{\perp}^2)^{1/2}$.

2.2 Magnetization plateau: H_c^{\pm}

To determine parameters characterizing the magnetization plateaux at $M = 0.5M_{sat}$, we use the continuum-limit bosonization treatment of the model (4). To obtain the continuum version of the Hamiltonian (4) we use the standard bosonization expression of the spin operators [39]

$$\tau_n^z = \sqrt{\frac{K}{\pi}} \partial_x \phi + \frac{(-1)^n}{\pi} \sin(\sqrt{4\pi K} \phi), \quad (7)$$

$$\tau_n^{\pm} = \frac{e^{-i\sqrt{\pi/K}\theta}}{\sqrt{2\pi}} \left[(-1)^n + \sin \sqrt{4\pi K} \phi \right], \quad (8)$$

where $\phi(x)$ and $\theta(x)$ are dual bosonic fields, $\partial_t \phi = v_s \partial_x \theta$ and the spin-stiffness parameter $K = \pi/2(\pi - \arccos \Delta)$. Using (7)-(8) we get the following bosonized Hamiltonian

$$H_{Bos} = \int dx \left\{ \frac{v_s}{2} [(\partial_x \phi)^2 + (\partial_x \theta)^2] - h_{eff}^0 \sqrt{\frac{K}{\pi}} \partial_x \phi + \frac{h_{eff}^1}{\pi a_0} \sin(\sqrt{4\pi K} \phi) \right\} \quad (9)$$

which is easily recognized as the standard Hamiltonian for the commensurate-incommensurate phase transition [40] and the Bethe ansatz [41]. We use these results to describe the magnetization plateau and transitions from a gapped (plateau) to the gapless Luttinger liquid phase.

Let us start our consideration from the case $h_{eff}^0 = 0$ corresponding to $H = J_{\perp} + J_{\parallel}/2$, where the Hamiltonian (9) reduces to the quantum sine-Gordon (SG) model with a massive term $\sim h_{eff}^1 \sin(\sqrt{4\pi K} \phi)$. From the exact solution of the SG model [42] it is known that the excitation spectrum is gapfull for $0 < K < 2$. At $1 < K < 2$ the excitation spectrum of the model consists of solitons and antisolitons with mass M , while for $0 < K < 1$ the

spectrum contains also soliton-antisoliton bound states ("breathers"). However for $1/2 < K < 1$ the soliton mass M remains the lowest excitation energy scale in the model. Below we will restrict our consideration by limiting cases of the isotropic antiferromagnetic and ferromagnetic ladder, corresponding to the case $\Delta = 1/2$ ($K = 3/4$) and $\Delta = -1/2$ ($K = 3/2$), respectively. Thus, in both considered cases the effective bosonized Hamiltonian is in the gapped regime with gap determined by the soliton mass M . Moreover from the exact solution [43] we can also get the exact scaling relation between the soliton mass physical M and its bare value $m_0 = \delta J_{\perp}$

$$M \simeq J_{\parallel} (\delta J_{\perp} / J_{\parallel})^{1/(2-K)}. \quad (10)$$

Thus at $h_{eff}^0 = 0$ the excitation spectrum of the system is gapped. In the ground state the field ϕ is pinned in one of the minima where $\langle 0 | \sin(\sqrt{4\pi K} \phi) | 0 \rangle = -1$, what corresponds (see Eq. (7)) to a long-range antiferromagnetic order in the ground state of the effective Heisenberg chain, i.e. to a phase of the initial ladder system, where odd rungs have a dominant triplet character and even rungs are predominantly singlets.

At $h_{eff}^0 \neq 0$ the very presence of the gradient term in the Hamiltonian (9) makes it necessary to consider the ground state of the sine-Gordon model in sectors with nonzero topological charge. The effective chemical potential $\sim h_{eff}^0 \partial_x \phi$ tends to change the number of particles in the ground state, what immediately implies that the vacuum distribution of the field ϕ will be shifted with respect of the minima which minimize the staggered part. This competition between contributions of the smooth and staggered components of the magnetic field is resolved as a continuous phase transition from a gapped state at $|h_{eff}^0| < M$ to a gapless Luttinger liquid phase at $|h_{eff}^0| > M$, where M is the soliton mass [40]. This condition immediately gives two additional critical values of the magnetic field

$$H_c^{\pm} = J_{\perp} + J_{\parallel}/2 \pm M, \quad (11)$$

and respectively the width of the magnetization plateau given by

$$H_c^+ - H_c^- \simeq 2J_{\parallel} (\delta J_{\perp} / J_{\parallel})^{1/(2-K)}. \quad (12)$$

It is straightforward to get, that in the case of a ladder with antiferromagnetic legs, the width of the magnetization plateau scales as $\delta^{4/5}$ while in the case of a ladder with ferromagnetic legs as δ^2 .

In order to investigate the detailed behavior of the ground state magnetic phase diagram and to test the validity of the picture obtained from continuum-limit bosonization treatment, below in this paper we present results of numerical calculations using the Lanczos method of exact diagonalizations for finite ladders.

3 Numerical results

In this section, to explore the nature of the spectrum and the quantum phase transition, we used Lanczos method to diagonalize numerically ladders with length up to $L = 14$.

3.1 The Energy Gap

First, we have computed the three lowest energy eigenvalues of ladders with antiferromagnetic (ferromagnetic) legs $J_{\parallel} = 1.0(-1.0)$ and different values of the rung exchanges $J_{\perp}(n)$. To get the energies of the few lowest eigenstates we consider ladders with periodic boundary conditions on legs.

In Fig.1, we present results of these calculations for the rung exchanges $J_{\perp}^0 = 11/2, \delta = 1/11$ and ladder sizes $L = 8, 10$. We define the excitation gap as a gap to the first excited state. As it can be seen in Fig.1, in the considered limit of strong on-rung exchange, this difference is characterized by the indistinguishable (within the used numerical accuracy) dependence on the ladder length and shows an universal linear decrease with increasing magnetic field.

At $H = 0$ the spectrum model is gapped for all cases (ferromagnetic and antiferromagnetic legs). For $H \neq 0$ the energy gap decreases linearly with H and vanishes at H_{c1} . This is the first level crossing between the ground-state energy and the first excited state energy. The spectrum remains gapless for $H_{c1} < H < H_c^-$ and once again becomes gapped for $H > H_c^-$. The spin gap, which appears at $H > H_c^-$, first increases with the external uniform magnetic field, but then starts to decrease, and again vanishes at H_c^+ . With more increasing field $H > H_c^+$, the spectrum remains gapless up to the critical saturation field H_{c2} . Finally, at $H > H_{c2}$ the gap opens again and for a sufficiently large field becomes proportional to H . In the regions $H_{c1} < H < H_c^-$ and $H_{c1} < H < H_{c2}$, the two lowest states cross each other $N/2$ times, which causes gapless regimes in the thermodynamic limit $N \rightarrow \infty$. These level crossings lead to incommensurate effects that manifest themselves in the oscillatory behavior of the response functions.

Let us now comment the numerical method which we use to extract critical values of the magnetic field in the thermodynamic limit ($L \rightarrow \infty$) from the finite ladder exact diagonalizations data. In an infinite system the critical point corresponds to a value of the magnetic field at which the energy gap vanishes. Since, in the case of finite systems the gap remains finite, we use the phenomenological renormalization group (PRG) method (see for details Ref.44) to obtain values of the critical fields. The phenomenological renormalization group equation for the energy gap $G(L, H)$ is written as

$$(L + 2)G(L + 2, H') = LG(L, H). \quad (13)$$

At the quantum critical point, $LG(L, H)$ should be size independent for large enough systems in which the contribution from irrelevant operators is negligible. This allows to determine critical points very accurately. We define

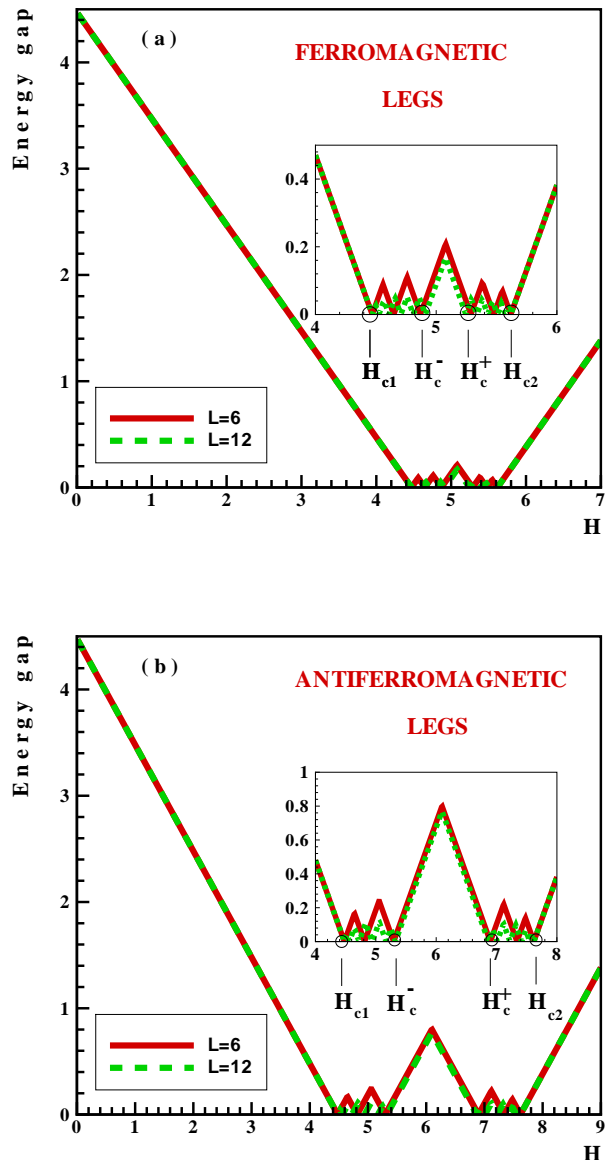


Fig. 1. Difference between the energy of the first excited state and the ground state energy as a function of the magnetic field H , for ladder with rung exchange $J_{\perp} = 11/2, \delta = 1/11$ and with (a) ferromagnetic legs $J_{\parallel} = -1.0$ (b) antiferromagnetic legs $J_{\parallel} = 1.0$, including different ladder lengths $L = 8, 10$.

$H_c(L, L + 2)$ as L -dependent fixed point of PRG equation and then it is extrapolated to the thermodynamic limit in order to estimate H_c . At the first step we plot the curve $LG(L, H)$ versus H for system sizes L and $L + 2$. These curves cross at a certain value $H_c(L, L + 2)$ which is determined as a finite size critical point. The thermodynamic critical point H_c is obtained by extrapolating $H_c(L, L + 2)$ to $L \rightarrow \infty$. Figure 2 shows the extrapolation procedure of the transition points for the ladder with antiferromagnetic legs and rung-exchange parameters $J_{\perp} = 11/2$ and

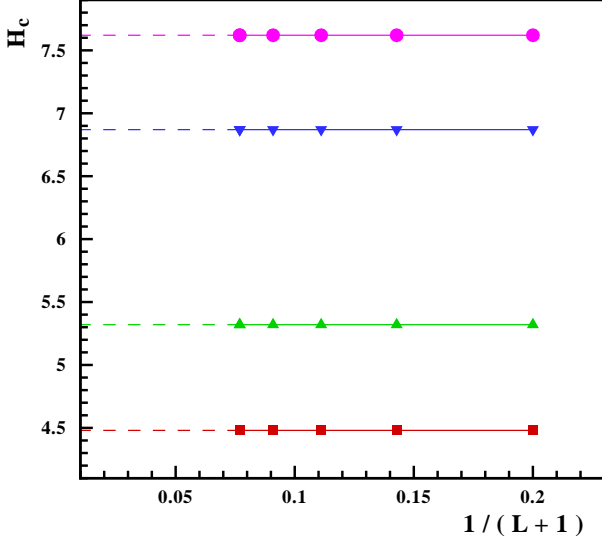


Fig. 2. Fixed points $H_c(L, L+2)$ of the PRG equation for the energy gap, plotted versus $1/(L+1)$, for $J_{\parallel} = 1.0$, $J_{\perp} = 11/2$, $\delta = 1/11$ and different ladder lengths $L = 4, 6, 8, 10, 12, 14$. The values of $H_c(L, L+2)$ for five pairs of system sizes $(L, L+2) = (4, 6), (6, 8), (8, 10), (10, 12)$, and $(12, 14)$ are represented in the figure.

$\delta = 1/11$. Obtained by this method values of critical are

$$H_{c_1} = 4.48 \pm 0.01, \quad H_{c_2} = 7.62 \pm 0.01, \quad (14)$$

$$H_c^- = 5.32 \pm 0.01, \quad H_c^+ = 6.87 \pm 0.01. \quad (15)$$

Analogously in the case of the ladder with ferromagnetic legs we obtain the following set of critical parameters

$$H_{c_1} = 4.47 \pm 0.01, \quad H_{c_2} = 5.62 \pm 0.01, \quad (16)$$

$$H_c^- = 4.89 \pm 0.01, \quad H_c^+ = 5.26 \pm 0.01. \quad (17)$$

One can easily check that the obtained values for critical field obtained from the finite ladder studies are very close to the values predicted analytically.

3.2 Magnetization curve

To study the magnetic order of the ground state of the system, we start with the magnetization process. First, we have implemented the Lanczos algorithm on finite ladders to calculate the lowest eigenstate. The magnetization along the field axis is defined as

$$M^z = \frac{1}{L} \sum_{n=1}^L \langle Gs | (S_{1,n}^z + S_{2,n}^z) | Gs \rangle, \quad (18)$$

where the notation $\langle Gs | \dots | Gs \rangle$ represent the ground state expectation value. In Fig. 3, we have plotted M^z as a function of the magnetic field H , and for a ladder with (a) ferromagnetic and (b) antiferromagnetic legs and with

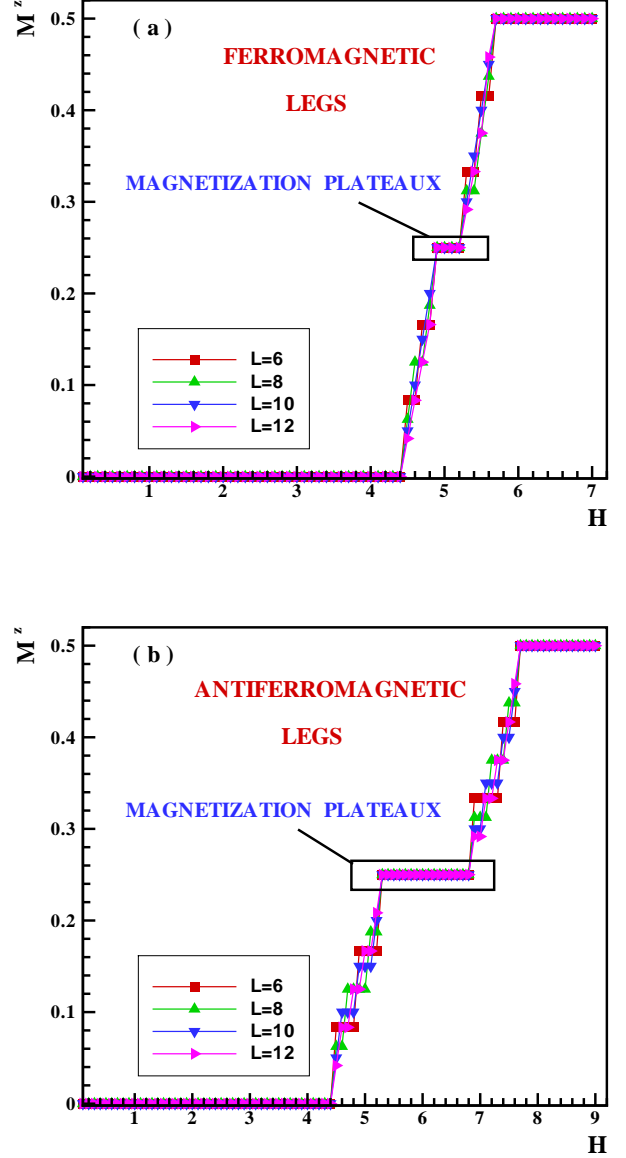


Fig. 3. a. The magnetization along field M^z as a function of the applied magnetic field H for (a) ferromagnetic ladder $J_{\parallel} = -1.0$ (b) antiferromagnetic ladder $J_{\parallel} = 1.0$, including different ladder lengths $L = 6, 8, 10, 12$.

ring exchange parameters $J_{\perp} = 11/2$, $\delta = 1/11$ and different lengths $L = 6, 8, 10, 12$.

As it is clearly seen in Fig. 3 besides the standard rung-singlet and saturation plateaus at $H < H_{c_1}$ and $H > H_{c_2}$ respectively observed in the case of ladders with uniform rung exchange [9,10], we observe a plateau at $M = 0.5M_{sat}$. Observed oscillations of the magnetization at $H_{c_1} < H < H_c^-$ and $H_c^+ < H < H_{c_2}$ result from the level crossing between the ground and the first excited states of this model in the gapless phases. Usually, in order to give an estimation of the width of magnetization

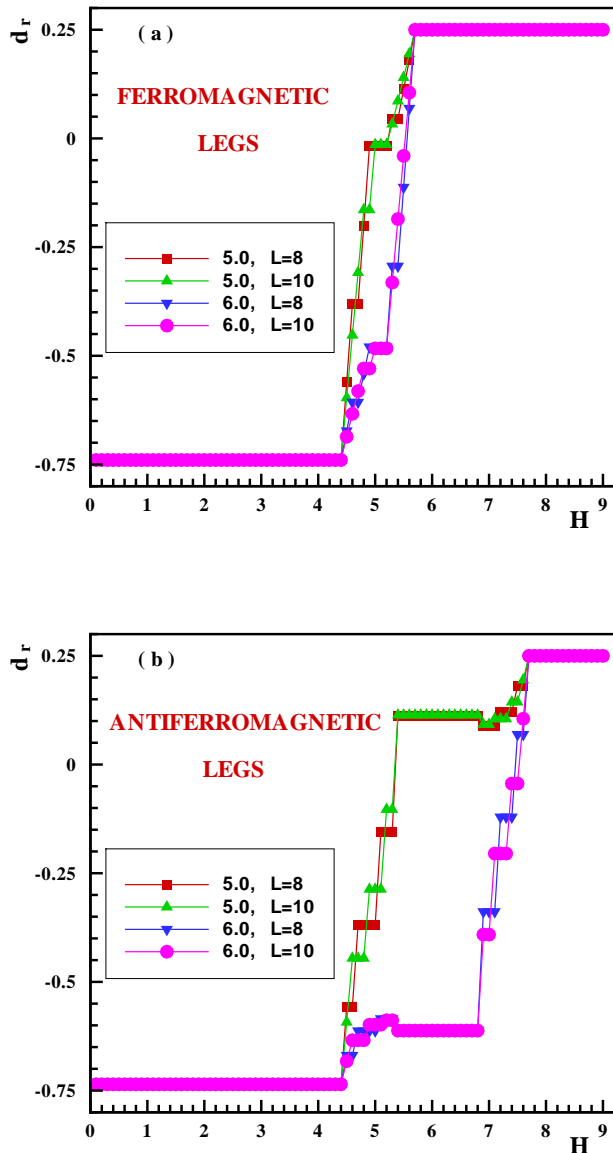


Fig. 4. The on-rung spin correlation functions for odd ($J_{\perp}^{-} = 5.0$) and even ($J_{\perp}^{+} = 6.0$) rungs as a function of the applied field H for $L = 8, 10$ lengths with rung exchange parameters $J_{\perp} = 11/2, \delta = 1/11$ with (a) ferromagnetic ($J_{\parallel} = -1.0$) and (b) antiferromagnetic legs ($J_{\parallel} = 1.0$).

plateau in the thermodynamic limit, the size scaling of its width is performed [18]. We also perform the similar analysis for selected values of the exchange parameters and found that the size of the plateau interpolates to finite value with $L \rightarrow \infty$.

An additional insight into the nature of different phases can be obtained studying the intra-rung correlations. We define the on-rung spin correlation function (rung dimer-

ization order parameter) for even and odd sites, as

$$d_r^e = \frac{2}{L} \sum_m \langle Gs | \mathbf{S}_{1,2m} \cdot \mathbf{S}_{2,2m} | Gs \rangle \quad (19)$$

and

$$d_r^o = \frac{2}{L} \sum_n \langle Gs | \mathbf{S}_{1,2m+1} \cdot \mathbf{S}_{2,2m+1} | Gs \rangle, \quad (20)$$

taking sum over even or odd sites, respectively. In Fig. 4 we have plotted the d_r^e and d_r^o as a function of the magnetic field H for the ladder of lengths $L = 8, 10$ with (a) ferromagnetic and (b) antiferromagnetic legs and the rung exchange parameters $J_{\perp} = 11/2, \delta = 1/11$. As it is seen from this figure, at $H < H_{c1}$ spins on all rungs are in a singlet state $d_r^e = d_r^o \simeq -0.75$, while at $H > H_{c2}$, d_r is slightly less than the saturation value $d_r^e = d_r^o \sim 1/4$ and the ferromagnetic long-range order along the field axis is present. Deviation from the saturation values $-3/4$ and $1/4$ reflects the effect of quantum fluctuations. However, in the considered case of strong rung-exchanges and high critical fields quantum fluctuations are substantially suppressed and calculated averages of on-rung spin correlations are very close to their nominal values.

On the other hand, for intermediate values of the magnetic field, at $H_{c1} < H < H_{c2}$ the data presented in Fig. 4 gives us a possibility to trace the mechanism of singlet-pair melting with increasing magnetic field. As it follows from Fig. 4 at H slightly above H_{c1} spin singlets pairs start to melt in all rungs simultaneously and almost with the same intensity. This effect is more profound in the case of ladder with ferromagnetic legs (Fig. 4.a) where the on-rung spin correlation functions increase almost parallel for even and odd rungs. With further increase of H melting of weak rungs gets more intensive, however at $H = H_c^{-}$ the process of melting stops. As it is seen in Fig. 4.b weak rungs are polarized, however their polarization is far from the saturation value $d_r^o \simeq 0.1$, while the strong rungs still manifest strong on-site singlet features with $d_r^e \simeq -0.62$. This effect is much weaker in the case of ferromagnetic legs in accordance with previous results. Moratorium on melting stops at $H = H_c^{+}$, however for $H > H_c^{+}$ strong rungs start to melt more intensively while the polarization of weak rungs increases slowly. Finally at $H = H_{c2}$ both subsystems of rungs achieve an identical, almost fully polarized state. Note, that the almost symmetric fluctuations in on-rung correlations, increase in d_r^e at $H \leq H_c^{-}$ decrease in d_r^o at $H \geq H_c^{+}$ reflect the enhanced role of quantum fluctuations in the vicinity of quantum critical points.

To complete our description of the phase at magnetization plateau with $M = 0.5M_{sat}$ we have calculated the rung-spin distribution in the ground state

$$M_n^z = \frac{1}{2} \langle Gs | (S_{n,1}^z + S_{n,2}^z) | Gs \rangle. \quad (21)$$

In Fig. 5 we have plotted the spin distribution in the ground state of a ladder with rung-exchange parameters

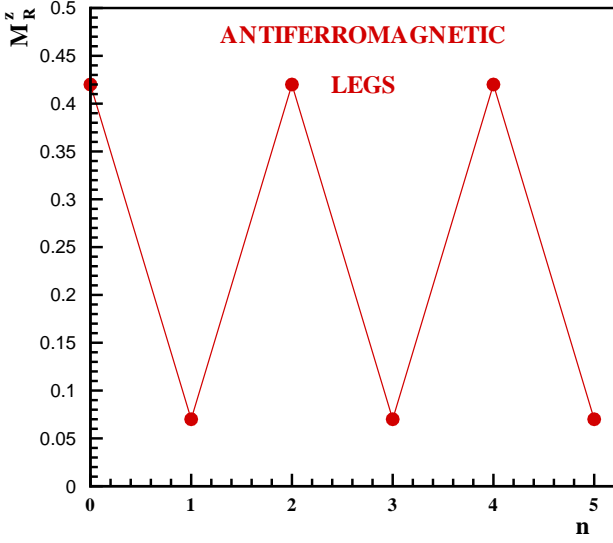


Fig. 5. The spin distribution in the GS as a function of the rung number "n" for magnetization corresponding to plateau at $M^z = 0.5M_{sat}^z$ and for rung exchanges $J_{\perp}^- = 5.0$ and $J_{\perp}^+ = 6.0$.

$J_{\perp} = 11/2, \delta = 1/11$ and antiferromagnetic legs as a function of the rung number "n" for a value of the magnetic field corresponding to the plateau at $M^z = 0.5M_{sat}^z$. To obtain an accurate estimate of the function M_n^z , we have calculated them from the Eq.(21) for system sizes of $L = 6, 8, 10, 12, 14$. The thermodynamic limit ($L \rightarrow \infty$) of the finite size results are obtained by extrapolation method and used for plotting. As we observe the system shows a well pronounced modulation of the on-rung magnetization, where magnetization on odd rung is larger than on even rungs. This distribution remains almost unchanged within the plateau for $H_c^- < H < H_c^+$.

3.3 Scaling properties of the magnetization plateau

To find an accurate estimate on the critical exponent characterizing width of the magnetization plateau on the parameter δ we have computed the critical fields H_c^{\pm} for the finite ladder systems with $L = 6, 8, 10, 12, 14, J_{\perp} = 10$ and different values of the parameter δ ($0.01 < \delta < 0.1$) and obtain their extrapolated values corresponding to the thermodynamic limit $L \rightarrow \infty$. In Fig. 6 we have plotted the log-log plot of the plateau width versus δ . Calculations has been performed both in the case of ladder with antiferromagnetic and ferromagnetic legs. We found that the best fit to our data (using the equation $H_c^+ - H_c^- \sim \delta^{\nu}$) yields $\nu = 1.82 \pm 0.02$ and $\nu = 0.87 \pm 0.01$ for the ladders with ferromagnetic and antiferromagnetic legs respectively.

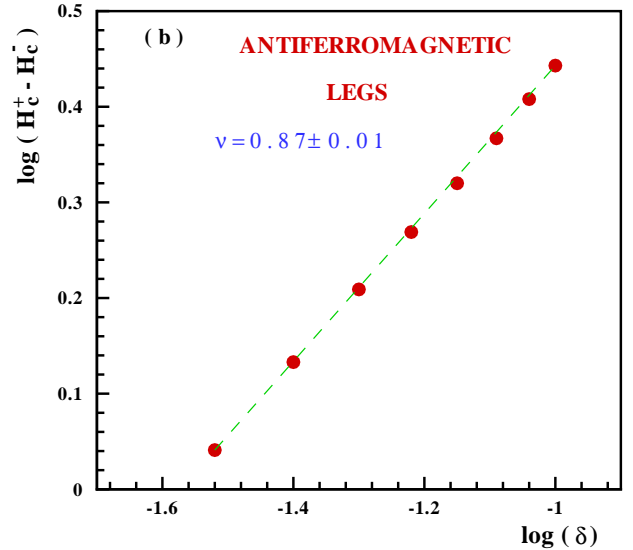
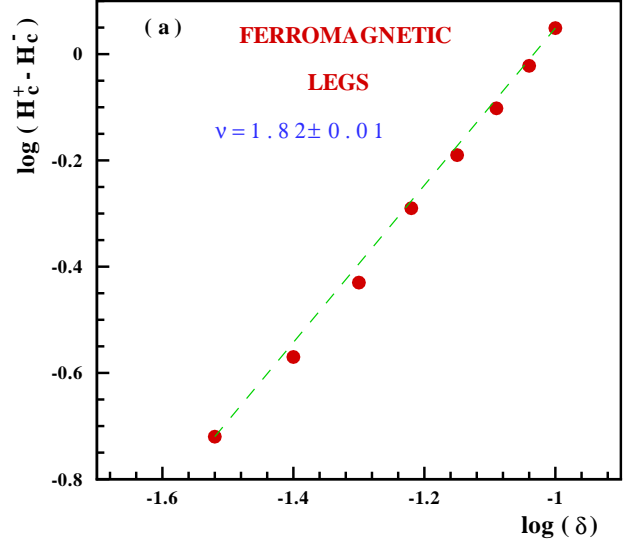


Fig. 6. Width of the magnetization plateau as a function of parameter δ for $0.01 < \delta < 0.1$ in the case of ladder with $J_{\perp} = 10.0$ and, (a) ferromagnetic ($J_{\parallel} = -1.0$) and (b) antiferromagnetic ($J_{\parallel} = 1.0$) legs.

4 Conclusion

In this paper we have studied the elementary excitations and the magnetic ground state phase diagram of a spin $S = 1/2$ two-leg ladder with alternating rung-exchange $J_{\perp}(n) = J_{\perp} [1 + (-1)^n \delta]$ using the continuum limit bosonization studies and the Lanczos method of numerical diagonalizations for ladders up to $L = 14$. We have shown that the rung-exchange alternation leads to generation of a gap in the excitation spectrum of the system at magnetization equal to the half of its saturation value. As a result of this new energy scale formation the magneti-

zation curve of the system $M(H)$ exhibits a plateau at $M = 0.5M_{sat}$. The width of the plateau, is proportional to the excitation gap and scales as δ^ν , where critical exponent $\nu = 0.87 \pm 0.01$ in the case of a ladder with isotropic antiferromagnetic legs and $\nu = 1.82 \pm 0.01$ in the case of a ladder with isotropic ferromagnetic legs. We have also calculated the magnetic field dependence of the on-rung spin-spin correlation functions. Comparison of these data for weak and strong rungs gave us an excellent description of the dynamics of the magnetization process in the case of ladder with non-equal rungs.

In a standard way we estimate the magnetic condensation energy as $E_{mag}(\delta) - E_{mag}(0) \sim -\delta^{2\nu}$. In the harmonic approximation the lattice deformation energy (per rung) can be estimated as $E_{def} \sim \delta^2$. Therefore we can conclude, that in the case of antiferromagnetic ladder, where $2\nu = 1.64 < 2$, the spontaneous appearance of an alternating rung exchange as a spin-Peierls instability during the magnetization process at $M = 0.5M_{sat}$ is possible.

5 Acknowledgments

It is our pleasure to thank T. Vekua for fruitful discussions. This work has been supported by the GNSF through the grant No. ST06/4-018. GIJ also acknowledges support through the research program of the SFB 608 funded by the DFG.

References

1. H. Bethe, Z. Phys. **71**, 205 (1931).
2. "Quantum Magnetism" Edited by U. Schollwöck, J. Richter, D.J.J. Farnell and R.F. Bishop, (Lect. Notes in Phys. **645**, Springer, Berlin 2004.)
3. S. Suchdev, Nature Physics **4**, 173 (2008).
4. T. Giamarchi, Ch. Rüegg, and O. Tchernyshyov, Nature Physics **4**, 198 (2008).
5. For a review see E. Dagotto, Rep. Prog. Phys. **62**, 1525 (1999); E. Dagotto and T.M. Rice, Science **271**, 618 (1996).
6. H.J. Schulz, Phys. Rev. B **34**, 6372, (1986).
7. I. Affleck, J. Phys. Condens. Matter **1**, 3047 (1991).
8. D.G. Shelton, A.A. Nersesyan and A.M. Tsvelik, Phys. Rev. B **53**, 8521 (1996).
9. C.A. Hayward, D. Poilblanc, and L.P. Lévy, Phys. Rev. B **54**, R12649 (1996).
10. R. Chitra and T. Giamarchi, Phys. Rev. B **55**, 5816 (1997).
11. D. C. Cabra, A. Honecker, and P. Pujol, Phys. Rev. Lett. **79**, 5126 (1997); *ibid* Phys. Rev. B **58**, 6241 (1998).
12. F. Mila, Eur. Phys. J. B **6**, 201 (1998).
13. K. Totsuka, Phys. Rev. B **57** 3454 (1998).
14. M. Usami and S. I. Suga, Phys. Rev. B **58**, 14401 (1998).
15. T. Giamarchi and A. M. Tsvelik, Phys. Rev. B **59**, 11398 (1999).
16. M. Hagiwara, H. A. Katori, U. Schollwöck, and H.-J. Mikeska, Phys. Rev. B **62**, 1051 (2000).
17. X. Wang and L. Yu, Phys. Rev. Lett. **84**, 5399 (2000).
18. M. E. Zhitomirsky, A. Honecker and O. A. Petrenko, Phys. Rev. Lett. **85**, 027207 (2000).
19. T. Hikihara and A. Furusaki Phys. Rev. B **63**, 134438 (2001)
20. S. Wessel, M. Olshanii, and S. Haas, Phys. Rev. Lett. **87**, 206407 (2001)
21. Y.-J. Wang, F. H. L. Essler, M. Fabrizio, and A. A. Nersesyan, Phys. Rev. B **66**, 024412 (2002).
22. Y.-J. Wang Phys. Rev. B **68**, 214428 (2003).
23. T. Vekua, G.I. Japaridze, and H.-J. Mikeska, Phys. Rev. B **70**, 014425 (2004).
24. G.I. Japaridze, A. Langari and S. Mahdavifar, Jour. Phys. C: Cond. Matter **19** 076201 (2007).
25. G. Chaboussant and P. A. Crowell, L. P. Lévy, O. Piovesana, A. Madouri, and D. Mailly, Phys. Rev. B **55**, 3046 (1997).
26. G. Chaboussant, M.-H. Julien, Y. Fagot-Revurat, M. Hanson, L.P. Lévy, C. Berthier, M. Horvatic, and O. Piovesana, Europ. Phys. J. B **6**, 167 (1998).
27. G. Chaboussant, Y. Fagot-Revurat, M.-H. Julien, M. E. Hanson, C. Berthier, M. Horvatic, L. P. Lévy, and O. Piovesana, Phys. Rev. Lett. **80**, 2713 (1998).
28. D. Arcon, A. Lappas, S. Margadonna, K. Prassides, E. Ribera, J. Veciana, C. Rovira, R. T. Henriques, and M. Almeida, Phys. Rev. B **60**, 4191 (1999).
29. H. Mayaffre, M. Horvatic, C. Berthier, M.-H. Julien, P. Ségransan, L. Lévy, and O. Piovesana, Phys. Rev. Lett. **85**, 4795 (2000).
30. B. C. Watson, V. N. Kotov, M. W. Meisel, D. W. Hall, G. E. Granroth, W. T. Montfrooij, S. E. Nagler, D. A. Jensen, R. Backov, M. A. Petruska, G. E. Fanucci, and D. R. Talham, Phys. Rev. Lett. **86**, 5168 (2001).
31. M.C. Cross and D.S. Fisher, *Phys. Rev. B* **19**, 402 (1979)
32. G.I. Japaridze and E. Pogossyan, Jour. Phys. C: Cond. Matter **18** 9297 (2006).
33. M. Oshikawa and J. Affleck, Phys. Rev. Lett. **79**, 28832886 (1997); *ibid* Phys. Rev. B **60**, 1038 (1999).
34. F. H. L. Essler and A. M. Tsvelik Phys. Rev. B **57**, 10592-10597 (1998).
35. J.-B. Fouet, O. Tchernyshyov, and F. Mila Phys. Rev. B **70**, 174427 (2004).
36. S. A. Zvyagin, A. K. Kolezhuk, J. Krzystek, and R. Feynherm, Phys. Rev. Lett. **95**, 027207 (2004).
37. S. Mahdavifar, Eur. Phys. J. B **55**, 371-376 (2007).
38. A. Luther and I. Peschel, Phys. Rev. B **12**, 3908 (1975).
39. A.O. Gogolin, A.A. Nersesyan and A.M. Tsvelik, *Bosonization and strongly correlated systems*, Cambridge University Press, Cambridge (1998).
40. G.I. Japaridze and A.A. Nersesyan, JETP Pis'ma **27** 356 (1978); [JETP Lett. **27**, 334 (1978)]; *ibid*. J. Low Temp. Phys. **37** 95 (1979); V.L. Pokrovsky and A.L. Talapov Phys. Rev. Lett. **42**, 65 (1979).
41. G.I. Japaridze, A.A. Nersesyan, and P.B. Wiegmann, Nucl. Phys. B **230**, 511 (1984).
42. R.F. Dashen, B. Hasslacher and A. Neveu, Phys. Rev. D **10** 3424 (1975); A. Takhtadjan and L.D. Faddeev, Sov. Theor. Math. Phys., **25**, 147 (1975).
43. Al. B. Zamolodchikov, Int. J. Mod. Phys. **A10** 1125 (1995).
44. M. N. Barber in *Phase Transitions and Critical Phenomena*, edited by C. Domb and J. L. Lebowitz (Academic Press, New York, 1983) v. **8**, 146.